

## **DISCLAIMER**

**This report was prepared as an account of work sponsored by an agency of the United States Government. Neither the United States Government nor any agency thereof, nor any of their employees, makes any warranty, express or implied, or assumes any legal liability or responsibility for the accuracy, completeness, or usefulness of any information, apparatus, product, or process disclosed, or represents that its use would not infringe privately owned rights. Reference herein to any specific commercial product, process, or service by trade name, trademark, manufacturer, or otherwise does not necessarily constitute or imply its endorsement, recommendation, or favoring by the United States Government or any agency thereof. The views and opinions of authors expressed herein do not necessarily state or reflect those of the United States Government or any agency thereof. Reference herein to any social initiative (including but not limited to Diversity, Equity, and Inclusion (DEI); Community Benefits Plans (CBP); Justice 40; etc.) is made by the Author independent of any current requirement by the United States Government and does not constitute or imply endorsement, recommendation, or support by the United States Government or any agency thereof.**

## Final Report

### *Project Title:*

**“Production of High Specific Activity  $^{155}\text{Tb}$ ,  $^{161}\text{Tb}$  and  $^{203}\text{Pb}$  for Research and Clinical Applications: Effective Target Design, Target Material Recycling and Radioisotope Separation”**

**Award #: DE-SC0022079**

### **Submitted by**

University of Washington  
4333 Brooklyn Ave NE  
Seattle, WA 98195-9472

### **University of Washington Principal Investigator**

Yawen Li, PhD  
Department of Radiation Oncology  
206-543-1405  
[liyw@uw.edu](mailto:liyw@uw.edu)

### **Co-Principal Investigators and Institutions on Project**

**University of Missouri**  
Heather M Hennkens, Ph.D. (**Lead PI**)  
[HennkensH@missouri.edu](mailto:HennkensH@missouri.edu)

**Brookhaven National Laboratory**  
Cathy S. Cutler, Ph.D. (**BNL PI**)  
[ccutler@bnl.gov](mailto:ccutler@bnl.gov)

Dmitri G. Medvedev, Ph.D. (**BNL Co-PI**)  
[dmedvede@bnl.gov](mailto:dmedvede@bnl.gov)

### **Report Provided to:**

Ethan Balkin, Ph.D.  
Isotope R&D Program Manager  
U.S. Department of Energy  
Office of Science Isotope Program  
301-903-3613  
[Ethan.Balkin@science.doe.gov](mailto:Ethan.Balkin@science.doe.gov)

Nov, 2024

This project is a trilateral collaboration between the University of Missouri (MU), Brookhaven National Laboratory (BNL) and the University of Washington (UW) and this **final report** provides a summary of the technical progress from UW.

## WORK-SCOPE HIGHLIGHTS

The submitted proposal described two research objectives for producing high specific activity radionuclides using reactor and accelerator technologies that would greatly expand options for theranostics in research and medical applications with the focuses being (1) Production of high specific activity terbium-155 ( $^{155}\text{Tb}$ ) and terbium-161 ( $^{161}\text{Tb}$ ) and (2) Evaluation of alternate methods of production and purification for high specific activity lead-203 ( $^{203}\text{Pb}$ ). Due to DOE Isotope Program's request to reduce the scope of the grant and advice to remove the  $^{203}\text{Pb}$  project, no research was conducted for the second research objective. The third objective involves graduate student and postdoctoral fellow education and training in support of workforce development in nuclear sciences.

At UW, our efforts focused on specific tasks to (1) compare the  $^{153}\text{Eu}(\alpha,2n)^{155}\text{Tb}$  and  $^{155}\text{Gd}(\alpha,4n)^{155}\text{Dy} \rightarrow ^{155}\text{Tb}$  reactions for production of  $^{155}\text{Tb}$ , (2) develop a durable  $^{153}\text{Eu}_2\text{O}_3$  target for production of  $^{155}\text{Tb}$ , (3) collaborate with Dr. Heather Hennkens on development of separation methods for isolating  $^{155}\text{Tb}$  from irradiated  $^{153}\text{Eu}_2\text{O}_3$  targets, and (4) provide training for graduate students and postdoctoral fellows in isotope production and separations.

## UW TASKS AND KEY ACCOMPLISHMENTS

### Task 1. Compare the $^{153}\text{Eu}(\alpha,2n)^{155}\text{Tb}$ and $^{155}\text{Gd}(\alpha,4n)^{155}\text{Dy} \rightarrow ^{155}\text{Tb}$ reactions for production of $^{155}\text{Tb}$ .

#### Key Accomplishments:

1. Designed and prepared natural abundance and enriched  $\text{Eu}_2\text{O}_3$  and  $\text{Gd}_2\text{O}_3$  targets for the evaluation of production rates and radionuclidic and radioisotopic purity.

A machinist/engineer at UW Medical Cyclotron Facility assisted our group in designing a new target holder compatible with the new automated target station developed and fabricated by the cyclotron team. This new two-piece target holder features a bottom piece with a well for pressing target material using a die and a laboratory hydraulic press, and a top piece designed to hold the target window for beam degradation and prevent sputtering. Importantly, the top piece can be easily attached or removed using custom-made tools, streamlining the removal of the irradiated target pellet for dissolution. With minor modifications to the well depth, the target holder can potentially be adapted for other pressed powder targets.

A Postdoc Fellow and a graduate student from the UW Physics Department prepared the targets by pressing high purity aluminum foils (or graphite powder) and a desired amount of natural abundance or enriched  $\text{Eu}_2\text{O}_3$  or  $\text{Gd}_2\text{O}_3$  powder into the bottom of the target holder sequentially. The aluminum foil and graphite powder were used to stop the beam. The prepared targets were covered with a thin silicon (Si) window or pyrolytic graphite sheet (PGS) to degrade the beam to the desired energy. The desired thicknesses of the target window,  $\text{Eu}_2\text{O}_3/\text{Gd}_2\text{O}_3$  layer, high purity aluminum foil/graphite layer were calculated using SRIM/TRIM.

Short irradiations (10-15 min) at an  $\alpha$ -beam current of 1  $\mu\text{A}$  were conducted to determine the production rates for  $^{155}\text{Tb}$  and other co-produced radioisotopes. The results are compared with production rates predicted using TENDL-2017 cross sections as shown in Tables 1 and 2.

**Table 1a.** Comparison of predicted and observed production rates of  $^{155}\text{Tb}$  and co-produced Tb radioisotopes on natural abundance  $\text{Eu}_2\text{O}_3$  targets.

| Nuclide | 24-18 MeV |            | 26-20 MeV |            | 28-22 MeV |            |
|---------|-----------|------------|-----------|------------|-----------|------------|
|         | Predicted | Experiment | Predicted | Experiment | Predicted | Experiment |
|         |           |            |           |            |           |            |

|                                       | ( $\mu\text{Ci}/\mu\text{Ah}$ ) |
|---------------------------------------|---------------------------------|---------------------------------|---------------------------------|---------------------------------|---------------------------------|---------------------------------|
| <b><math>^{152}\text{Tb}</math></b>   | 0                               | 0                               | 0                               | 0                               | 0                               | 0                               |
| <b><math>^{152m}\text{Tb}</math></b>  | 0                               | 0                               | 0                               | 0                               | 0                               | 0                               |
| <b><math>^{153}\text{Tb}</math></b>   | 35.5                            | 24.9                            | 53.7                            | 26.2                            | 66.1                            | 53.2, 59.0                      |
| <b><math>^{154}\text{Tb}</math></b>   | 9.91                            | 3.41                            | 7.85                            | 3.11                            | 7.35                            | 1.51, 1.41                      |
| <b><math>^{154m1}\text{Tb}</math></b> | 10.3                            | 78.5                            | 5.79                            | 86.8                            | 3.41                            | 52.7, 45.3                      |
| <b><math>^{154m2}\text{Tb}</math></b> | -                               | 2.41                            | -                               | 2.59                            | -                               | 1.81, 1.59                      |
| <b><math>^{155}\text{Tb}</math></b>   | 17.1                            | 22.6                            | 25.7                            | 24.2                            | 30.2                            | 37.0, 48.4                      |
| <b><math>^{156}\text{Tb}</math></b>   | 1.08                            | 1.89                            | 0.77                            | 2.19                            | 0.59                            | 0.97, 1.11                      |

**Table 1b.** Comparison of predicted and observed production rates of  $^{155}\text{Tb}$  and co-produced Tb radioisotopes on enriched [ $^{153}\text{Eu}$ ] $\text{Eu}_2\text{O}_3$  targets.

| Nuclide                               | 26-20 MeV                                    |   | 28-22 MeV                                    |   | 30-24 MeV                                    |   |
|---------------------------------------|--|---|--|---|--|---|
|                                       | Predicted<br>( $\mu\text{Ci}/\mu\text{Ah}$ ) | Experiment<br>( $\mu\text{Ci}/\mu\text{Ah}$ ) | Predicted<br>( $\mu\text{Ci}/\mu\text{Ah}$ ) | Experiment<br>( $\mu\text{Ci}/\mu\text{Ah}$ ) | Predicted<br>( $\mu\text{Ci}/\mu\text{Ah}$ ) | Experiment<br>( $\mu\text{Ci}/\mu\text{Ah}$ ) |
| <b><math>^{152}\text{Tb}</math></b>   | 0  | 0   | 0.04   | 0   | 0.29   | 0   |
| <b><math>^{152m}\text{Tb}</math></b>  | 0  | 0   | 6.48   | 0   | 127  | 0   |
| <b><math>^{153}\text{Tb}</math></b>   | 1.38   | 0.99  | 1.70   | 1.84  | 2.23   | 2.07  |
| <b><math>^{154}\text{Tb}</math></b>   | 0.09   | 0   | 10.3   | 0.79  | 51.3   | 1.68  |
| <b><math>^{154m1}\text{Tb}</math></b> | 0.09   | 1.87  | 8.58   | 15.6  | 38.5   | 5.22  |
| <b><math>^{154m2}\text{Tb}</math></b> | -  | 0.20  | -  | 0.65  | -  | 71.4  |
| <b><math>^{155}\text{Tb}</math></b>   | 48.6   | 51.4  | 57.2   | 94.6  | 70.0   | 70.3  |
| <b><math>^{156}\text{Tb}</math></b>   | 1.45   | 3.27  | 1.20   | 2.51  | 1.45   | 1.39  |

**Table 2.** Comparison of predicted and observed production rates of  $^{155}\text{Dy}$ ,  $^{155}\text{Tb}$  and co-produced  $^{157}\text{Dy}$  and  $^{156}\text{Tb}$  on enriched [ $^{155}\text{Gd}$ ] $\text{Gd}_2\text{O}_3$  targets.

| 47-37 MeV                           |       |  |   |
|-------------------------------------|-------|--|---|
|                                     |       | Predicted<br>( $\mu\text{Ci}/\mu\text{Ah}$ ) | Experiment<br>( $\mu\text{Ci}/\mu\text{Ah}$ ) |
| <b><math>^{155}\text{Dy}</math></b> | EOB   | 1260   | 1020  |
|                                     | ~50 h | 38.0   | 23.6  |
| <b><math>^{155}\text{Tb}</math></b> | EOB   | 2.0  | 29.6  |
|                                     | ~50 h | 78.8   | 73.0  |
| <b><math>^{157}\text{Dy}</math></b> | EOB   | 368  | 484   |
|                                     | ~50 h | 5.20   | 5.2   |
| <b><math>^{156}\text{Tb}</math></b> | EOB   | 4.0  | 12  |
|                                     | ~50 h | 2.8  | 9.2   |
| 45-35 MeV                           |       |  |   |
|                                     |       | Predicted<br>( $\mu\text{Ci}/\mu\text{Ah}$ ) | Experiment<br>( $\mu\text{Ci}/\mu\text{Ah}$ ) |
| <b><math>^{155}\text{Dy}</math></b> | EOB   | 864  | 604   |
|                                     | ~50 h | 18.4   | 17.2  |
| <b><math>^{155}\text{Tb}</math></b> | EOB   | 1.0  | 17.2  |
|                                     | ~50 h | 55.6   | 50.8  |
| <b><math>^{157}\text{Dy}</math></b> | EOB   | 424  | 508   |
|                                     | ~50 h | 6  | 7.2   |

|                      |   |      |  |
|----------------------|---|------|--|
| <sup>156</sup> Tb    | EOB   | 3.2  | 7.2  |
|                      | ~50 h   | 2.4  | 6.4  |
| <b>41.5-31.5 MeV</b> |   |      |  |
|                      | <b>Predicted</b><br>( $\mu\text{Ci}/\mu\text{Ah}$ ) |      | <b>Experiment</b><br>( $\mu\text{Ci}/\mu\text{Ah}$ ) |
| <sup>155</sup> Dy    | EOB   | 332  | 216  |
|                      | ~50 h   | 10   | 5.6  |
| <sup>155</sup> Tb    | EOB   | 0.3  | 5.6  |
|                      | ~50 h   | 20.8 | 14.4   |
| <sup>157</sup> Dy    | EOB   | 596  | 696  |
|                      | ~50 h   | 8.4  | 5.6  |
| <sup>156</sup> Tb    | EOB   | 1.6  | 6.4  |
|                      | ~50 h   | 1.2  | 4.8  |

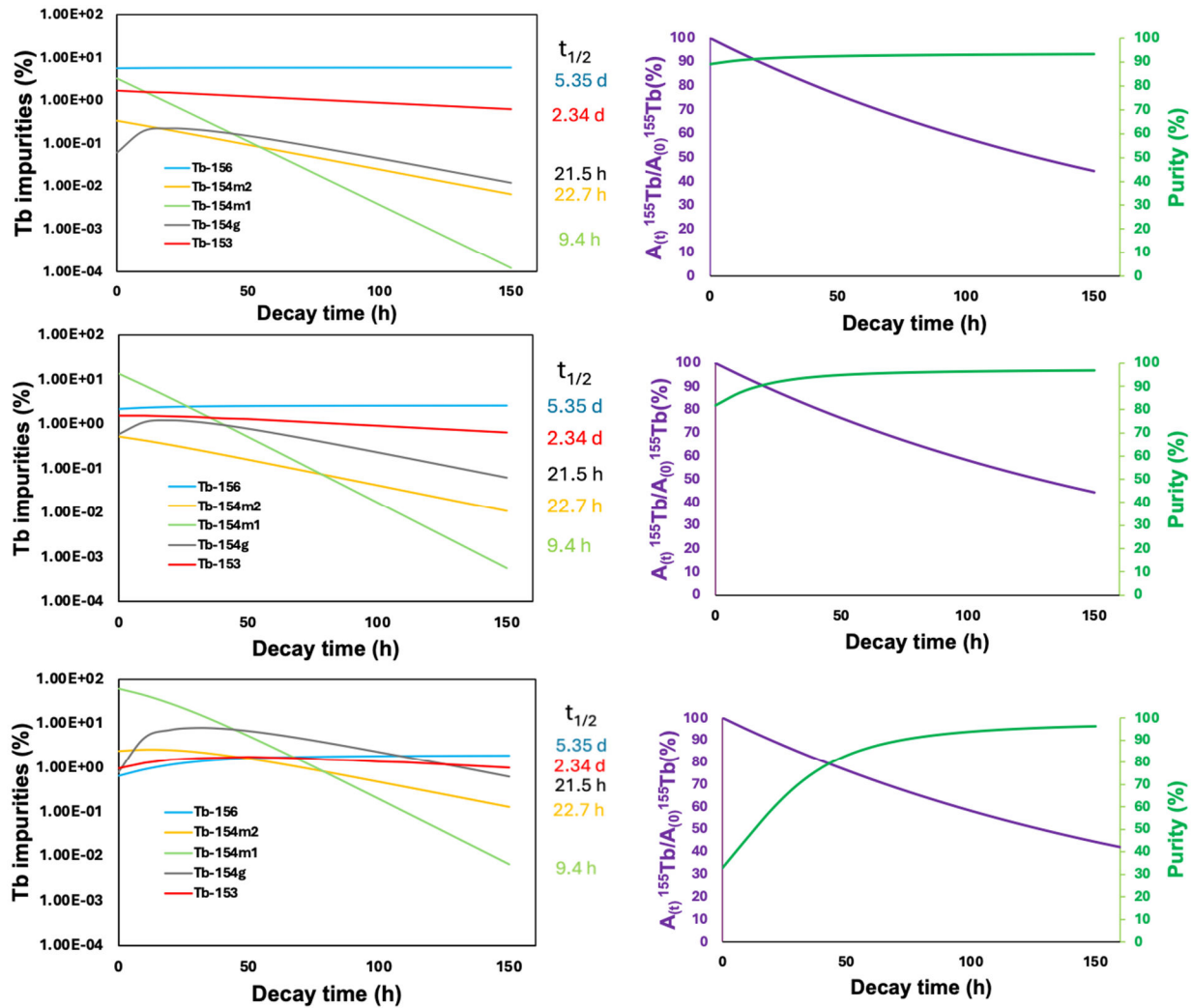
2. Identified the optimal energy windows for the  $\alpha$ -beam to achieve highest <sup>155</sup>Tb production rates and radionuclidic and radioisotopic purity via the  $^{153}\text{Eu}(\alpha,2n)^{155}\text{Tb}$  and  $^{155}\text{Gd}(\alpha,4n)^{155}\text{Dy} \rightarrow ^{155}\text{Tb}$  reactions.

Table 3 illustrates that when an enriched <sup>153</sup>Eu target is irradiated by a 28 MeV  $\alpha$ -beam, which exits the target at 22 MeV, a production rate of 94.6  $\mu\text{Ci}/\mu\text{Ah}$  can be achieved via the  $^{153}\text{Eu}(\alpha,2n)$  reaction. After a 100-h decay time removing majority of the short-lived radioisotopic impurities (i.e. <sup>153</sup>, <sup>154g</sup>, <sup>154m1</sup>, <sup>154m2</sup>Tb), a high radioisotopic purity of 96.2% can be achieved, which is the highest radioisotopic purity of <sup>155</sup>Tb reported in the literature to date to our knowledge. However, this decay period does not help reduce the <sup>156</sup>Tb ( $t_{1/2} = 5.35$  d) impurity due to its similar half-life to <sup>155</sup>Tb. The preliminary data obtained suggest we could potentially produce  $\sim 65$  mCi of <sup>155</sup>Tb with a radioisotopic purity of >95% at 60 hours post EOB via a 20-h irradiation at a beam current of 50  $\mu\text{A}$ . This quantity and purity will make it possible to support use of <sup>155</sup>Tb in preclinical and clinical research. The percentage of impurities and purity of <sup>155</sup>Tb as a function of time in Figure 1.

**Table 3.** Summary of production rates of  $^{153}\text{Eu}(\alpha,2n)^{155}\text{Tb}$  v.s  $^{155}\text{Gd}(\alpha,4n)^{155}\text{Dy} \rightarrow ^{155}\text{Tb}$  and <sup>155</sup>Tb purity observed after irradiations conducted across the listed  $\alpha$ -beam windows.

| Nuclear reaction  | Energy window (MeV) | Production rate at EOB <sup>a</sup> |  | <sup>155</sup> Tb Purity, 100 h (%) |
|---|---------------------|-------------------------------------|--|-------------------------------------|
| <sup>153</sup> Eu( $\alpha,2n$ )<br><sup>155</sup> Tb<br>(98.77% enrichment)  | 26-20               | 51.4                                |  | 93.1                                |
|   | 28-22               | 94.6                                |  | 96.2                                |
|   | 30-24               | 70.3                                |  | 93.9                                |
| <sup>155</sup> Gd( $\alpha,4n$ )<br><sup>155</sup> Dy<br>(90.266% enrichment) |                     | <sup>155</sup> Dy                   | <sup>155</sup> Tb, ~50 h post EOB <sup>c</sup> |                                     |
|   | 47-37               | 1020                                | 73.0   | 88.8 <sup>b</sup>                   |
|   | 45-35               | 603                                 | 51.4   | 88.8 <sup>b</sup>                   |
|   | 41.5-31.5           | 216                                 | 13.5   | 75 <sup>b</sup>                     |

<sup>a</sup>Values are in  $\mu\text{Ci}/\mu\text{Ah}$ . <sup>b</sup>Purity of <sup>155</sup>Tb without 2-step purification. <sup>157</sup>Dy was the main impurity observed. <sup>c</sup>The activity of <sup>155</sup>Tb reaches its maximum at 39.6 h post EOB, but HPGe analyses were conducted at 50 h post EOB due to normal working hours.



**Figure 1.** Variation in  $^{155}\text{Tb}$  purity and impurity levels over time for enriched  $[^{153}\text{Eu}]\text{Eu}_2\text{O}_3$  targets irradiated by 26-20 MeV (A), 28-22 MeV (B) and 30-24 MeV (C)  $\alpha$ -beams, respectively.

The  $^{155}\text{Gd}(\alpha, 4n)^{155}\text{Dy} \rightarrow ^{155}\text{Tb}$  reaction potentially can provide an even higher radioisotopic purity through a 2-step purification process, however, the product rate in the 47-37 MeV energy window is about 20% lower than that of the  $^{153}\text{Eu}(\alpha, 2n)$  in the 28-22 MeV energy window. Also, the target material, enriched  $^{155}\text{Gd}$  oxide costs about twice as much as  $^{153}\text{Eu}$  oxide, and a  $^{155}\text{Gd}$  target needs twice as much of it compared to  $^{153}\text{Eu}$  under the optimized production parameters (i.e. target thickness and beam energy).

## Task 2. Develop a durable $^{153}\text{Eu}_2\text{O}_3$ target for production of $^{155}\text{Tb}$ .

### **Key Accomplishments:**

1. Demonstrated irradiation of a  $^{153}\text{Eu}_2\text{O}_3$  target for 2 h at an average  $\alpha$ -beam current of 10  $\mu\text{A}$  with a peak beam current of 13  $\mu\text{A}$ .

An essential step for achieving large-scale production of  $^{155}\text{Tb}$  is to develop a durable target that can withstand  $\alpha$ -irradiations at a high beam current for multiple hours. Because Eu metal rapidly oxidizes in air and spontaneously reacts with water, we have focused on the development of a pressed powder target using  $[^{153}\text{Eu}]\text{Eu}_2\text{O}_3$ .  $\text{Eu}_2\text{O}_3$  has a high melting point of 2,350 °C and low thermal conductivity of 2.45 W/m·K. Because our targets are cooled by water running in the back of the target, heat transfer within the target assembly is key to prevent target failures due to overheating.

Carbon-based substances (like carbon fiber, carbon nanotubes, graphene, and diamond), metallic elements (such as Ag, Al, and Cu), and ceramics ( $\text{Al}_2\text{O}_3$ , SiC, AlN, and BN), have been extensively used as thermal-conductive fillers, to increase the thermal conductivity of polymer matrices. We designed and fabricated a series of targets made of  $\text{Eu}_2\text{O}_3$  and other filler materials that have both high melting point and high thermal conductivity. Examples of the filler materials are shown in Table 4. To prepare these targets, we first press a piece of high purity Al foil into the target holder as a low activation beam stop. Then an appropriate amount of  $\text{Eu}_2\text{O}_3$  is mixed carefully with a small amount of the filler material (5% wt%), which is subsequently pressed into the target holder. Finally, the target pellet is covered using a thin pyrolytic graphene sheet (PGS). The thermal contact between the different layers within the target is another critical aspect that affects the overall thermal conductance. In the current target design, a graphite-based adhesive is used at the Al/ $\text{Eu}_2\text{O}_3$  and  $\text{Eu}_2\text{O}_3$ /PGS interfaces.

Scanning electron microscopy (SEM) and energy dispersive X-ray (EDS) imaging has been used to assess the microstructure of the target pellet of  $\text{Eu}_2\text{O}_3$ /nanodiamonds. (Figure 2) The presence of clusters of nanodiamonds suggests that the target preparation process can be further refined to generate a more homogeneous mixture of  $\text{Eu}_2\text{O}_3$  and nanodiamonds. Preliminary test irradiations performed for pressed  $\text{Eu}_2\text{O}_3$  targets containing nanodiamonds (5% wt%) using a 30 MeV  $\alpha$ -beam demonstrated that these targets could withstand  $\alpha$ -beam currents of up to 13  $\mu\text{A}$  during testing. In a production run, we achieved a 2 h irradiation at an average beam current of 10  $\mu\text{A}$ , producing a total of 839  $\mu\text{Ci}$   $^{155}\text{Tb}$  at EOB. The reduced production rate is attributed to the lower beam energy reaching the  $[\text{Eu}^{153}]\text{Eu}_2\text{O}_3$  target, caused by energy loss through the adhesive used to enhance thermal contact. It is anticipated that a significantly higher production rate of  $^{155}\text{Tb}$  could be achieved by optimizing the  $\alpha$ -beam energy.

**Table 4.** Physical properties of example thermal-conductive fillers.

| Filler material  | Thermal conductivity (W/m·K) | Melting point (°C) | Density (g/cm <sup>3</sup> ) |
|------------------|------------------------------|--------------------|------------------------------|
| Nanodiamond      | ~1000                        | ~3500              | 3.5                          |
| Microdiamond     | 1000-2000                    | ~3500              | 3.5                          |
| BN               | 751                          | 2973               | 2.1 (h-BN);<br>3.45 (c-BN)   |
| Carbon nanotubes | 2000-3000                    | 3550               | 1.3-1.4                      |
| SiC              |                              | 2830               | 3.16                         |

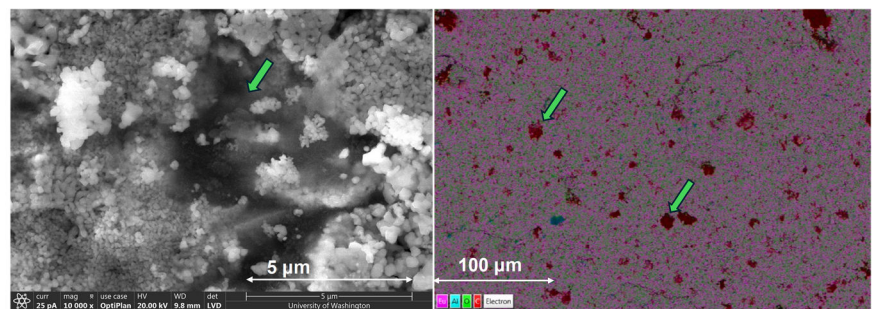


**Figure 2.** SEM (left) and SEM/EDS overlay (right) images of  $\text{Eu}_2\text{O}_3$  with 5% wt% dispersed nanodiamonds (left). Elemental composition as shown in the SEM/EDS overlay image: C (red), O (green), Eu (pink), and Al (cyan). Green arrows point to clusters of nanodiamonds.

Although not within the funded scope of work, based on the results obtained, we started a new collaboration with scientists at BNL to conduct thermal contact resistance measurements. With help from the BNL team, we have performed thermal testing and analyses on  $\text{Eu}_2\text{O}_3$  targets used for optimizing production parameters to determine the thermal contact conductance of the internal layers within the targets, up to and including the back wall of the target. This information is critical for target design, as these targets are cooled by conduction heat transfer to the water-cooled back wall, external to the target. A BNL custom-built thermal conductance test system was used for those experiments. The system is comprised of a vacuum chamber with feedthroughs that supply cooling, via a semi-cyrogenic chiller with a cold head, as well as electrical penetrations for heating elements and resistance temperature detectors (RTDs). By carefully attaching the target on the cold and heated sides and providing heat on one side with cooling on the other, a series of steady state and thermal transient tests cycles can be performed.

The temperature vs. time data is recorded for each detector and each thermal cycle is then brought into a transient thermal analysis using finite element analysis (FEA) software. The combination of test data and the FEA analysis allows for the final determination of the thermal conductance values from each layer within the target.

Staff from UW MCF and our research group visited BNL in July 2023 to observe and learn thermal contact conductance measurement and analysis. Since then we have assembled a similar apparatus at UW. Recently a UW Mechanical Engineering junior has worked with other senior team members in our group on building models using the COMSOL software, setting up and testing the new apparatus, and conducting thermal contact resistance measurements.

### **Task 3. Collaborate with Dr. Heather Hennkens (MU) on development of separation methods for isolating $^{155}\text{Tb}$ from irradiated $^{153}\text{Eu}_2\text{O}_3$ targets.**

The development of separation methods for isolating  $^{155}\text{Tb}$  from irradiated  $^{153}\text{Eu}_2\text{O}_3$  targets has progressed with a focus on the target configuration described in Task 2. The UW team evaluated a method for removing bulk of Eu by the reduction of  $\text{Eu}^{3+}$  by zinc (Zn) metal powder in an acidic solution, followed by precipitation as  $\text{EuSO}_4$ , as well as the LN resin for the separation of  $^{155}\text{Tb}$  from residual Eu target material. Separation studies were conducted using non-irradiated  $\text{Eu}_2\text{O}_3$  targets and irradiated  $^{153}\text{Eu}_2\text{O}_3$  targets.

For example, in one study, a  $^{153}\text{Eu}_2\text{O}_3$  target was irradiated at an average beam current of 10  $\mu\text{A}$  for 1 hour using the 30 MeV  $\alpha$ -beam, producing 617  $\mu\text{Ci}$  of  $^{155}\text{Tb}$  at EOB. The irradiated target was dissolved in 5 mL of concentrated HCl and heated to 95°C to ensure complete dissolution. Eu debulking via precipitation as europium sulfate, facilitated by the addition of an optimized amount of Zn powder, removed 98.5% of the target material. Subsequent separation using a column packed with an optimized amount of LN resin achieved an 80% recovery of  $^{155}\text{Tb}$ . Quality control analysis by HPGe indicated a product purity of approximately 96% at 100 hours post-EOB. These results highlight the potential of the proposed process for efficient  $^{155}\text{Tb}$  production.

In a collaboration with Dr. Heather Hennkens (MU), an electroamalgamation- and chromatography-based Eu/Tb separation method has been developed. Initial studies at MU were conducted using  $^{161}\text{Tb}$  as a surrogate for  $^{155}\text{Tb}$  to optimize electroamalgamation conditions and the subsequent chromatographic process which uses three different extraction resins. To further demonstrate the developed process, an irradiated  $^{153}\text{Eu}_2\text{O}_3$  target containing 940  $\mu\text{Ci}$  of  $^{155}\text{Tb}$  was shipped to MU, where the separation of  $^{155}\text{Tb}$  from the irradiated  $^{153}\text{Eu}_2\text{O}_3$  target was successfully demonstrated. The details of these studies are provided in the MU final technical report submitted by Dr. Heather Hennkens.

### **Task 4. Provide training for graduate students and postdoctoral fellows in isotope production and separations.**

Three postdoctoral fellows, one graduate student and an undergraduate student worked on various aspects of the project, including target design and preparation, thermal analysis, gamma spectroscopy, separation studies, etc. The postdoctoral fellows and graduate student also presented their research progress our bimonthly trilateral institution Zoom project meetings, coordinated and organized by Dr. Heather Hennkens (MU), as well as national and international conferences (e.g. iSRS and ACS meetings). Two of the postdoctoral fellows now employed at TerraPower and the third postdoctoral fellow has been promoted to a Research Scientist within our research group. Additionally, a graduate student from MU visited our research group for two weeks for cross-training. During the visit, he toured the cyclotron facility and worked with members in our research group on  $^{153}\text{Eu}_2\text{O}_3$  target preparation and separation.

## **DELIVERABLES**

Manuscript under review

Patrick Bokolo, Madhushan Serasinghe, Marina Kuchuk, Jim Guthrie, Mary Embree, Stacy Wilder, Dmitri G. Medvedev, Cathy S. Cutler, D. Scott Wilbur, Yawen Li, Carolyn J. Anderson, Silvia S. Jurisson, Heather M. Hennkens, Production and Purification of Research Scale  $^{161}\text{Tb}$  Using Cation-Exchange Semi-Preparative HPLC for Radiopharmaceutical Applications, *Radiochimica Acta*

Manuscript in preparation

Anster Charles, Peter de Roos, Robert Smith, Marissa Kranz, Sean Tanzey, Cathy Cutler, Dmitri G. Medvedev, Carolyn J. Anderson, Silvia S. Jurisson, Heather M. Hennkens, D. Scott Wilbur, Yawen Li, An Evaluation of the Production of  $^{155}\text{Tb}$  in High Specific Activity via Alpha-Irradiation of Enriched  $^{153}\text{Eu}]\text{Eu}_2\text{O}_3$  and  $^{155}\text{Gd}]\text{Gd}_2\text{O}_3$  Targets, *Applied Radiation and Isotopes*

Abstracts

1. Madhushan Serasinghe, Patrick Bokolo, Ritin Kamboj, John D. Lydon, Jim Guthrie, Steven Kelley, D. Scott Wilbur, Yawen Li, Dmitri G. Medvedev, Cathy S. Cutler, Carolyn J. Anderson, Silvia S. Jurisson, Heather M. Hennkens, Development of methods for isolation of radioactive terbium from europium and target material recycling, Gordon Research Conference on Metals in Medicine, Andover, New Hampshire; June 23-28, 2024
2. Patrick Bokolo, Madhushan Serasinghe, Leo Manson, John D. Lydon, Jim Guthrie, Mary Embree, Steven Kelley, Dmitri G. Medvedev, Cathy S. Cutler, D. Scott Wilbur, Yawen Li, Carolyn J. Anderson, Silvia S. Jurisson, Heather M. Hennkens, Recycling Method Development in Support of Cost-Effective  $^{161}\text{Tb}$  Production, Gordon Research Conference on Metals in Medicine, Andover, New Hampshire; June 23-28, 2024
3. Anster Charles, Peter de Roos, Sean Tanzey, Bob Smith, Eric Dorman, Marissa Kranz, D. Scott Wilbur, Dmitri G. Medvedev, Cathy S. Cutler, Carolyn J. Anderson, Silvia S. Jurisson, Heather Hennkens, Yawen Li, Evaluation of alpha irradiation of  $^{153}\text{Eu}]\text{Eu}_2\text{O}_3$  and  $^{155}\text{Gd}]\text{Gd}_2\text{O}_3$  targets for producing high specific activity  $^{155}\text{Tb}$ , the ACS Spring 2024 National Meeting & Exposition, New Orleans, LA & Hybrid, United States, March 17-21, 2024
4. Madhushan Serasinghe, Patrick Bokolo, Ritin Kamboj, John D. Lydon, James Guthrie, D. Scott Wilbur, Yawen Li, Dmitri G. Medvedev, Cathy S. Cutler, Carolyn J. Anderson, Silvia S. Jurisson, Heather M. Hennkens, Research scale separation of radioterbium using electro-amalgamation and extraction chromatography methods, the ACS Spring 2024 National Meeting & Exposition, New Orleans, LA & Hybrid, United States, March 17-21, 2024
5. Michael Chimes, Pavithra Kankamalage, Dmitri Medvedev, Cathy Cutler, D. Scott Wilbur, Yawen Li, Carolyn J. Anderson, Silvia S. Jurisson, Heather M. Hennkens, Separation of high specific activity  $^{161}\text{Tb}$  and  $^{155}\text{Tb}$  from proton irradiated  $^{nat}\text{Dy}$  foils, the ACS Spring 2024 National Meeting & Exposition, New Orleans, LA & Hybrid, United States, March 17-21, 2024
6. Patrick Bokolo, Madhushan Serasinghe, Leonard Manson, John D. Lydon, Mary Embree, Dmitri Medvedev, Cathy S. Cutler, D. Scott Wilbur, Yawen Li, Carolyn J. Anderson, Silvia S. Jurisson, Heather M. Hennkens, A Comparison of Cation Exchange and Extraction Column-based Chromatography Methods for Isolating MURR Produced  $^{161}\text{Tb}$ , 25th International Symposium of Radiopharmaceutical Sciences, Honolulu, Hawaii, United States, May 22 – 26, 2023
7. Madhushan Serasinghe, Patrick Bokolo, Ritin Kamboj, John D. Lydon, Jim Guthrie, D. Scott Wilbur, Yawen Li, Dmitri Medvedev, Cathy S. Cutler, Carolyn J. Anderson, Silvia S. Jurisson, Heather M. Hennkens, Development of an effective electro-amalgamation technique for debulking of Eu(III) from Eu(III)/Tb(III) mixtures, 25th International Symposium of Radiopharmaceutical Sciences, Honolulu, Hawaii, United States, May 22 – 26, 2023
8. Anster Charles, Sean Tanzey, Peter de Roos, Eric Dorman, Marissa Kranz, Bob Smith, Robert Emery, Dmitri Medvedev, Cathy S. Cutler, Carolyn J. Anderson, Silvia S. Jurisson, Heather M. Hennkens, D. Scott Wilbur, Yawen Li, An Evaluation of the Production of High Specific Activity  $^{155}\text{Tb}$  via Alpha-Irradiation of Thick Natural  $\text{Eu}_2\text{O}_3$  and Enriched  $^{153}\text{Eu}]\text{Eu}_2\text{O}_3$  Targets, 25th International Symposium of Radiopharmaceutical Sciences, Honolulu, Hawaii, United States, May 22 – 26, 2023
9. Patrick Bokolo, Madhushan Serasinghe, Marina Kuchuk, Jim Guthrie, Mary Embree, Dmitri Medvedev, Cathy S. Cutler, D. Scott Wilbur, Yawen Li, Carolyn J. Anderson, Silvia S. Jurisson, Heather M. Hennkens, Isolation of Research Scale  $^{161}\text{Tb}$  for Medical Applications Using Cation-Exchange Semi-Preparative HPLC, National Organization for the Professional Advancement of Black

Chemists and Chemical Engineers (NOBCChE) Conference, Orlando, Florida, September 26-29, 2022